

AN IMPROVED NEARLY-ANALYTIC EXPONENTIAL TIME DIFFERENCE METHOD FOR SOLVING SEISMIC WAVE EQUATIONS

NAM YUN and CHOL SIM

*Institute of Mathematics, State Academy of Sciences, Pyongyang, D.P.R. Korea.
simchol@star-co.net.kp*

(Received July 11, 2018; revised version accepted December 12, 2019)

ABSTRACT

Yun, N. and Sim, C., 2020. An improved nearly-analytic exponential time difference method for solving seismic wave equations. *Journal of Seismic Exploration*, 29: 99-124.

We present an improved nearly-analytic exponential time difference (INETD) method, which is a version of the nearly-analytic exponential time difference (NETD) method proposed by Zhang. The NETD method is based on a combination of the exponential time difference (ETD) scheme with the nearly-analytic discrete (NAD) operator. In solving the acoustic and elastic wave equations, NETD first uses the NAD operator to approximate the high-order spatial differential operators, and then the resulting semi-discrete ODEs are solved by the ETD method. Because NETD is based on the structure of the Lie group method, it can achieve more accurate results than the classical methods. The main purpose of the present article is to improve the stability and the time accuracy in the original NETD method. To this end, we first derive an implicit ETD scheme and apply it to approximate the time derivatives instead of the explicit scheme in the original NETD method. For this new method, we analyze in detail its stability condition, the dispersion relation and the theoretical and numerical errors, and compare it with the NETD method. In addition, for the 2D case, using INETD, NETD and the fourth-order Lax-Wendroff correction (LWC) methods we simulate acoustic and elastic wave-fields, and compare numerical results for these different methods. Our theoretical analyses show that the stability condition of the INETD method is more relaxed than that of the original NETD method. The temporal accuracy of the INETD method is increased from second order in the original NETD method to third order, and spatial accuracy remains the same as that of the original. Moreover, the INETD method has the same computational costs and storage space as the NETD method and the numerical dispersion is less than the NETD method. The results of numerical experiments demonstrate the high efficiency of this method for acoustic and elastic wave modeling.

KEY WORDS: nearly-analytic discrete method, exponential time difference method, Lie group method, numerical dispersion, numerical approximations and analysis.

INTRODUCTION

This article contains a variation of the nearly-analytic exponential time difference (NETD) method. The NETD method is an effective numerical scheme for solving the acoustic and elastic wave equations, which is based on a combination of the exponential time difference (ETD) scheme to approximate the time derivatives and the nearly-analytic discrete (NAD) operator to approximate the space derivatives.

The development of effective and accurate numerical techniques has become increasingly meaningful for investigation of seismic waves in complicated and anisotropic media. There are many numerical methods available, including the finite element method (FEM), the finite difference method (FDM), the pseudospectral (PS) method, the reflectivity method, the boundary integral equation-discrete wavenumber method, the spectral element method, and so on. Each method has its inherent advantages and disadvantages (Yang et al., 2004). For example, FD methods have easy implementation, low-memory requirement, fast calculation and high parallelism (Kelly et al., 1976; Dablain, 1986; Wang et al., 2002). However, the FD suffers from serious numerical dispersion when too few spatial sampling points per wavelength are used or when models have large velocity contrasts between adjacent layers (Fei et al., 1995; Yang et al., 2002; Zheng et al., 2006). However, high-order methods or finer space grids can also be used to reduce the numerical dispersion, but there are also a lack of guarantee of a necessarily lower phase velocity error of the wave, and increases of memory requirements and CPU computation time. Meanwhile, the pseudospectral (PS) method (Huang et al., 1992; Kosloff et al., 1982, 1984; Fornberg, 1998) is attractive, but it requires the Fourier transform of wavefield, which is computationally expensive and has difficulty in handling sharp boundaries (Mizutani et al., 2000).

To effectively solve this problem, a nearly-analytic discrete operator was first introduced to approximate the high-order partial differential operators in seismic wave equations (Yang et al., 2003, 2004, 2006, 2007). This method can effectively suppress the numerical dispersion, and has fourth-order spatial accuracy. Based on the NAD approximation, many schemes have been developed (Yang et al., 2009, 2010a, b, 2012; Chen et al., 2010; Tong et al., 2013; Li et al., 2017), and each testifies to its superiority in suppressing numerical dispersions over conventional algorithms.

In recent years, NAD-type methods have been applied in wave propagation modeling in porous media with fluids (Yang et al., 2007, 2014) and seismic migration (Li et al., 2013; Xie et al., 2014; Feng et al., 2015). Also, schemes that combine geometric integration with the NAD method to solve seismic wave equations have been developed (Ma et al., 2011, 2014, 2015; Liu et al., 2017). The geometric integration method for solving ODEs is designed to preserve the qualitative properties of the original systems. These integration methods include the symplectic method, the symmetry method, the first integral preservation method (Hairer et al., 2006, and the references therein), the Lie group method (Munthe-Kaas, 1999; Iserles et al., 2000; Robert, 1991) and so on. Geometric integrations are shown to be superior to the general-purpose methods in some aspects, especially in long time computation, owing to their preservation of the qualitative properties. Thus, combining of geometric integrations with NAD may lead to decreases in numerical dispersion and numerical error over other classical methods.

Motivated by this fact, Zhang et al. (2014) developed a nearly-analytic exponential time difference (NETD) method. NETD uses an exponential time difference (ETD) scheme to approximate the time derivatives and the nearly-analytic discrete (NAD) operator to approximate the space derivatives. The ETD scheme used in this method can be also derived from the idea of the Lie group method. Therefore, the NETD method by combining the Lie group method with the NAD method to solve seismic wave equations effectively suppresses the numerical dispersion and preserves the qualitative properties of PDEs. Through theoretical and numerical analysis, they showed that NETD method provides more accurate results, has high computational efficiency, and a low memory requirement compared to the Lax-Wendroff correction (LWC) and the staggered-grid (SG) methods. However, the NETD method has some disadvantages; for example, its stability criterion is relatively compact and has only second-order time accuracy. It is important to improve the stability of the NETD method and increase its time accuracy for practical calculations.

From this view point, we focus on this problem. We present an improved NETD (INETD), for solving acoustic- and elastic-wave equations. The INETD scheme is composed of the following two steps: (i) Derivation a new implicit ETD scheme, (ii) Combination of the implicit ETD for the temporal discretization with the NAD method for the spatial discretization. This produces an improvement in the stability and the time accuracy over the NETD, because the explicit ETD scheme is used to approximate the time

derivatives in the NETD. In general, the implicit scheme has a good stability property, but it requires more expensive computations than the explicit scheme, because it solves the system of equations at every temporal step. We show that the INETD method needs the same computational costs and storage space as the NETD method. On the other hand, we find another possibility for improving the stability of the INETD method. It is to use the terms up to the third order in the truncated power series expansion used to explicitly solve the INETD system of linear equations. Our analysis shows it brings about a remarkable improvement in the stability of the method. On the whole, the our INETD method are shown to be superior to the FDM, the PS and the NETD methods in some aspects such as suppressing numerical dispersions, high accuracy, computational efficiency, a low memory and the improvement of stability.

This article is organized as follows. First, we review the basic NETD scheme for solving the acoustic wave equation in a 2D homogeneous medium. Then, we derive the INETD scheme. Next, we investigate in detail the properties of the INETD method. We derive the stability condition for the 1D and 2D cases. We estimate the theoretical and numerical errors of the INETD method, and compare against the NETD method. And then, we derive the dispersion relation and give the numerical dispersion results. Finally, for the 2D case we use the INETD, the original NETD and the fourth order LWC methods to simulate acoustic wave fields, and present some comparisons of numerical results for different methods. And then a homogeneous elastic model and a two-layer elastic model are further selected to investigate the computational validity of elastic wave-field simulations.

Our theoretical and numerical results show that the INETD is an improvement over the original NETD in stability, numerical error and numerical dispersion.

BASIC NEARLY-ANALYTIC EXPONENTIAL TIME DIFFERENCE (NETD) METHOD

In this section, we review and analyze the derivation of the original NETD method (Zhang et al., 2014) for solving the acoustic wave equation.

Exponential time difference method

Consider the stiff system

$$\frac{du}{dt} = \mathbf{L}u + \mathbf{N}(u, t) \quad , \quad (1)$$

where \mathbf{L} is a higher-order linear term and \mathbf{N} is a lower-order nonlinear term. To solve eq. (1), the equation is multiplied by an integrating factor

$$\frac{d}{dt} (\exp(-\mathbf{L}t)u) = \exp(-\mathbf{L}t)\mathbf{N}(u, t) \quad , \quad (2)$$

and then eq. (2) is integrated over a single temporal step of length τ ,

$$u^{n+1} = \exp(\mathbf{L}\tau)u^n + \exp(\mathbf{L}\tau) \int_0^\tau \exp(-\mathbf{L}s)\mathbf{N}(u(t_n + s), t_n + s)ds, \quad (3)$$

where u^n denote the numerical solution on the n -th time layer t_n . To approximate the integration in eq. (3), using the approximation as

$$\mathbf{N}(u(t_n + s), t_n + s) \approx \mathbf{N}(u^n, t_n) \quad , \quad (4)$$

the numerical scheme for solving eq. (1) is obtained as:

$$u^{n+1} = \exp(\mathbf{L}\tau)u^n + \mathbf{L}^{-1}(\exp(\mathbf{L}\tau) - \mathbf{I})\mathbf{N}(u^n, t_n) \quad . \quad (5)$$

Basic computational formulae

The acoustic wave equation in 2D homogeneous medium is written as

$$\frac{\partial^2 u}{\partial t^2} = c_0^2 \Delta u, \quad (6)$$

where u and c_0 are the displacement and the acoustic velocity, respectively,

and $\Delta = \frac{\partial^2}{\partial x^2} + \frac{\partial^2}{\partial z^2}$ is the Laplace operator. The same notations as that in

the basic NETD (Zhang et al., 2014) are used in our present study, i.e.,

$$w = \frac{\partial u}{\partial t}, \quad \mathbf{U} = \left(u, \frac{\partial u}{\partial x}, \frac{\partial u}{\partial z} \right)^T, \quad \mathbf{W} = \left(w, \frac{\partial w}{\partial x}, \frac{\partial w}{\partial z} \right)^T.$$

Eq. (6) can be rewritten as

$$\begin{cases} \frac{\partial \mathbf{U}}{\partial t} = \mathbf{W} \\ \frac{\partial \mathbf{W}}{\partial t} = c_0^2 \left(\frac{\partial^2 \mathbf{U}}{\partial x^2} + \frac{\partial^2 \mathbf{U}}{\partial z^2} \right). \end{cases} \quad (7)$$

The high-order spatial derivatives in eq. (7) are determined by the displacement \mathbf{U} and its gradients using the fourth-order NAD operator as shown in Appendix A of Zhang et al. (2014). Then eq. (7) can be transformed into an ODE system as follows:

$$\frac{d}{dt} \begin{pmatrix} \mathbf{U} \\ \mathbf{W} \end{pmatrix}_{j,k} = \begin{pmatrix} \mathbf{0} & \mathbf{I} \\ \mathbf{\Omega} & \mathbf{0} \end{pmatrix} \begin{pmatrix} \mathbf{U} \\ \mathbf{W} \end{pmatrix}_{j,k} + \tilde{\mathbf{N}}(\mathbf{U}, \mathbf{W})_{j,k}. \quad (8)$$

The first part of the right side of eq. (8) is a linear combination of u, w with its gradients at the grid point (x_j, z_k) , and the second part is a linear combination of u, w with its gradients at its neighboring grid points. \mathbf{I} is a 3×3 identity matrix and $\mathbf{\Omega}$ is a 3×3 matrix that depends on the spatial discrete operator. Using the notations

$$\mathbf{Y}_{j,k} = (\mathbf{U}, \mathbf{W})_{j,k}^T, \quad \text{and} \quad \tilde{\mathbf{L}} = \begin{pmatrix} \mathbf{0} & \mathbf{I} \\ \mathbf{\Omega} & \mathbf{0} \end{pmatrix}$$

and regarding $\tilde{\mathbf{N}}(\mathbf{Y}_{j,k})$ as a nonlinear function of $\mathbf{Y}_{j,k}$, eq. (8) can be rewritten as

$$\frac{d\mathbf{Y}_{j,k}}{dt} = \tilde{\mathbf{L}}\mathbf{Y}_{j,k} + \tilde{\mathbf{N}}(\mathbf{Y}_{j,k}) \quad , \quad (9)$$

Eq. (9) is rewritten as

$$\frac{d\mathbf{Y}}{dt} = \mathbf{L}\mathbf{Y} + \mathbf{N}(\mathbf{Y}) \quad , \quad (10)$$

where $\mathbf{Y} = (\mathbf{Y}_{j,k})$. Using the exponential time difference scheme (5) to solve eq. (10), Zhang et al. (2014) obtained a numerical scheme

$$\mathbf{Y}^{n+1} = \exp(\mathbf{L}\Delta t)\mathbf{Y}^n + \mathbf{L}^{-1}(\exp(\mathbf{L}\Delta t) - \mathbf{I})\mathbf{N}(\mathbf{Y}^n) \quad , \quad (11)$$

where Δt is the temporal step size. To improve the stability of the NETD method, by replacing \mathbf{Y}^n with $\frac{1}{2}(\mathbf{Y}^{n+1} + \mathbf{Y}^n)$, scheme (11) is reformed into an implicit scheme

$$\left(\mathbf{I} - \frac{1}{2}\mathbf{L}^{-1}(\exp(\mathbf{L}\Delta t) - \mathbf{I})\mathbf{N} \right) \mathbf{Y}^{n+1} = \left(\exp(\mathbf{L}\Delta t) + \frac{1}{2}\mathbf{L}^{-1}(\exp(\mathbf{L}\Delta t) - \mathbf{I})\mathbf{N} \right) \mathbf{Y}^n \quad . \quad (12)$$

To explicitly solve the system of linear equations in scheme (12), it is rewritten as

$$\mathbf{Y}^{n+1} = (\mathbf{I} + \mathbf{B} + \mathbf{B}^2) \left(\exp(\mathbf{L}\Delta t) + \frac{1}{2}\mathbf{L}^{-1}(\exp(\mathbf{L}\Delta t) - \mathbf{I})\mathbf{N} \right) \mathbf{Y}^n \quad , \quad (13)$$

by using the truncated power series expansion

$$(\mathbf{I} - \mathbf{B})^{-1} \approx \mathbf{I} + \mathbf{B} + \mathbf{B}^2 \quad , \quad (14)$$

where $\mathbf{B} = \frac{1}{2} \mathbf{L}^{-1} (\exp(\mathbf{L}\Delta t) - \mathbf{I}) \mathbf{N}$.

IMPROVED NEARLY-ANALYTIC EXPONENTIAL TIME DIFFERENCE (INETD) METHOD

Now take a closer look at the approximation (4) used in the original NETD method. The exponential time difference scheme (5) obtained by using the approximation (4) is explicit and has only second order accuracy, because of the use of low-order approximation (4). Therefore, the numerical scheme (11) also becomes explicit, which results in instability, and has second order accuracy in time.

In view of the above-mentioned points, we try to increase the stability and the time accuracy of the original NETD, using the following approximation instead of (4),

$$\mathbf{N}(u(t_n + s), t_n + s) \approx \mathbf{N}(u^n, t_n) + \frac{s}{\tau} (\mathbf{N}(u^{n+1}, t_{n+1}) - \mathbf{N}(u^n, t_n)) \quad , \quad (15)$$

to obtain the exponential time difference scheme

$$u^{n+1} = \exp(\mathbf{L}\tau)u^n + \frac{1}{\tau} (\mathbf{L}^{-1})^2 (\exp(\mathbf{L}\tau) - \mathbf{L}\tau - \mathbf{I}) \mathbf{N}^{n+1} + \frac{1}{\tau} (\mathbf{L}^{-1})^2 (\mathbf{L}\tau \exp(\mathbf{L}\tau) - \exp(\mathbf{L}\tau) + \mathbf{I}) \mathbf{N}^n, \quad (16)$$

where $\mathbf{N}^n = \mathbf{N}(u^n, t_n)$, and $\mathbf{N}^{n+1} = \mathbf{N}(u^{n+1}, t_n + \tau) = \mathbf{N}(u^{n+1}, t_{n+1})$. Using the exponential time difference scheme (16) to solve eq. (10), gives the numerical scheme

$$\mathbf{Y}^{n+1} = \exp(\mathbf{L}\Delta t) \mathbf{Y}^n + \frac{1}{\Delta t} (\mathbf{L}^{-1})^2 (\exp(\mathbf{L}\Delta t) - \mathbf{L}\Delta t - \mathbf{I}) \mathbf{N} \mathbf{Y}^{n+1} + \frac{1}{\Delta t} (\mathbf{L}^{-1})^2 (\mathbf{L}\Delta t \exp(\mathbf{L}\Delta t) - \exp(\mathbf{L}\Delta t) + \mathbf{I}) \mathbf{N} \mathbf{Y}^n. \quad (17)$$

Eq. (17) can be rewritten as follows:

$$\left(\mathbf{I} - \frac{1}{\Delta t} (\mathbf{L}^{-1})^2 (\exp(\mathbf{L}\Delta t) - \mathbf{L}\Delta t - \mathbf{I})\mathbf{N} \right) \mathbf{Y}^{n+1} = \left(\exp(\mathbf{L}\Delta t) + \frac{1}{\Delta t} (\mathbf{L}^{-1})^2 (\mathbf{L}\Delta t \exp(\mathbf{L}\Delta t) - \exp(\mathbf{L}\Delta t) + \mathbf{I})\mathbf{N} \right) \mathbf{Y}^n. \quad (18)$$

Now, following the original NETD method, we can solve the system of linear equations in scheme (18) explicitly. Let

$$\mathbf{C} := \frac{1}{\Delta t} (\mathbf{L}^{-1})^2 (\exp(\mathbf{L}\Delta t) - \mathbf{L}\Delta t - \mathbf{I})\mathbf{N}$$

and use the truncated power series expansion

$$(\mathbf{I} - \mathbf{C})^{-1} \approx \mathbf{I} + \mathbf{C} + \mathbf{C}^2 \quad . \quad (19)$$

Then, we can rewrite scheme (18) explicitly as

$$\mathbf{Y}^{n+1} = (\mathbf{I} + \mathbf{C} + \mathbf{C}^2) \left(\exp(\mathbf{L}\Delta t) + \frac{1}{\Delta t} (\mathbf{L}^{-1})^2 (\mathbf{L}\Delta t \exp(\mathbf{L}\Delta t) - \exp(\mathbf{L}\Delta t) + \mathbf{I})\mathbf{N} \right) \mathbf{Y}^n. \quad (20)$$

Comparing, we find that the INETD method (20) needs the same storage space and computational costs as the NETD method (13). For example, the total number of arrays required for computation in both is 12 for 1D and 18 for 2D in the acoustic content. There are differences in computational costs between the coefficient matrices of the NETD and the INETD schemes, but compared with the total computational costs this difference can be neglected, because there is no need to compute the coefficient matrix at each iteration, so it is sufficient to estimate it once before the iterations. Therefore, computational costs of two methods are the same. Also, the INETD method is an improvement over the original NETD method in both the stability and the computational accuracy in time, as verified in our theoretical analyses and numerical experiments below. The numerical dispersion error of the INETD method is less than that of the NETD method.

The exponential time difference scheme (16) used in the INETD method can be also obtained from the Lie group method. The Lie group method is the geometric integration method and preserves qualitative properties of differential equations.

STABILITY CRITERIA AND NUMERICAL DISPERSION ANALYSIS

Stability condition

To keep numerical calculation stable, the temporal increment Δt must satisfy the stability condition of the INETD method. Following the analysis process presented by Yang et al. (2006) and Liyd (1996), we obtain the stability condition of the INETD method for solving the acoustic wave equations in 1D and 2D. Through a series of mathematical operations, we obtain the following stability condition for the 1D homogeneous case,

$$\Delta t \leq \alpha_{\max} \frac{h}{c_0} \approx 0.5178 \frac{h}{c_0}, \quad (21)$$

where h denotes the space increment. For the 2D homogeneous case, the stability condition of the INETD method (20) under the condition $\Delta x = \Delta z = h$ is given by

$$\Delta t \leq \alpha_{\max} \frac{h}{c_0} \approx 0.3136 \frac{h}{c_0}. \quad (22)$$

Table 1. The approximate maximum Courant numbers of the original and improved methods.

| Method | NETD | INETD |
|-----------------------|--------|--------|
| α_{\max} (1-D) | 0.4132 | 0.5178 |
| α_{\max} (2-D) | 0.2583 | 0.3136 |

For comparison, Table 1 contains the approximate maximum Courant numbers of the NETD and INETD methods for 1D and 2D. From Table 1, we can see the stability condition of the INETD method is more relaxed than that of the NETD method.

Numerical dispersion analysis

In wavefield simulations, numerical dispersion (or grid dispersion) is the most significant numerical problem limiting the usefulness of point-wise discretization of wave equations. Following the analysis of previous work (Dablain, 1986; Lloyd, 1996; Yang et al., 2006), we obtain the dispersion relationship of the INETD method for 1D and 2D acoustic wave equations.

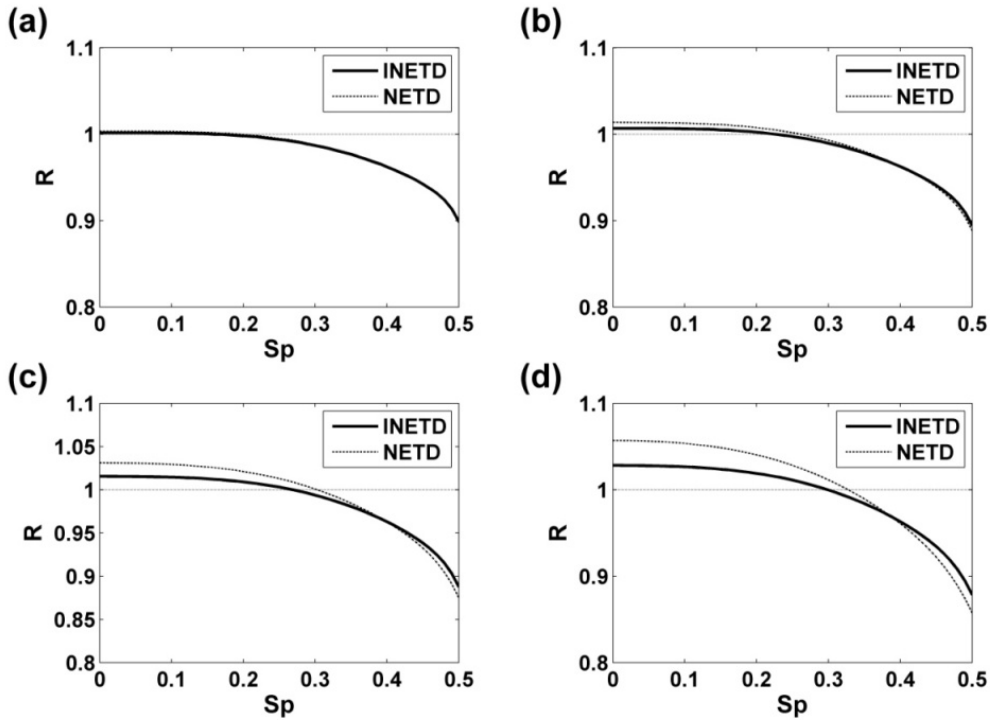


Fig. 1. The ratio R of the numerical velocity to the exact phase velocity versus the sampling rate S_p for the INETD and NETD methods for the 1D homogeneous case. The Courant numbers are **a** 0.1, **b** 0.2, **c** 0.3, and **d** 0.4, respectively .

Table 2. The average dispersive errors of the INETD and the original NETD methods for different Courant numbers for the 1D Case.

| Method | Courant number (α) | | | |
|--------|-----------------------------|-------|-------|-------|
| | 0.1 | 0.2 | 0.3 | 0.4 |
| INETD | 1.924 | 2.051 | 2.402 | 3.028 |
| NETD | 1.949 | 2.321 | 3.207 | 4.665 |

We define the spatial sampling ratio first proposed by Moszo et al. (2000) as $S_p = h/\lambda$, in which λ , denotes the wavelength. The dispersion ratio R is defined as $R = c_{num}/c_0$, in which c_{num} and c_0 denote the numerical and true velocities, respectively. $R = 1$ implies the method has no numerical dispersion. The dispersion relation as a function of the sampling rate (grid spacing per wavelength) is shown for the 1D case in Fig. 1. Table 2 shows the average numerical dispersive errors of the INETD and the original NETD methods for different Courant numbers (Fig. 1). The average numerical dispersive error is given by

$$\text{Error} = \frac{\int_0^{0.5} |1 - R| dS_p}{0.5} \times 100 (\%).$$

From Fig. 1 and Table 2, we can see the average dispersion error and the maximal dispersion error of the INETD method for the 1D case are less than that of the NETD method. Fig. 2 shows the average numerical dispersive errors of the INETD and the original NETD methods for different Courant numbers and various values of propagation angles in the 2D case. In Fig. 2 we observe that the average dispersion error of the INETD method is less than that of the NETD.

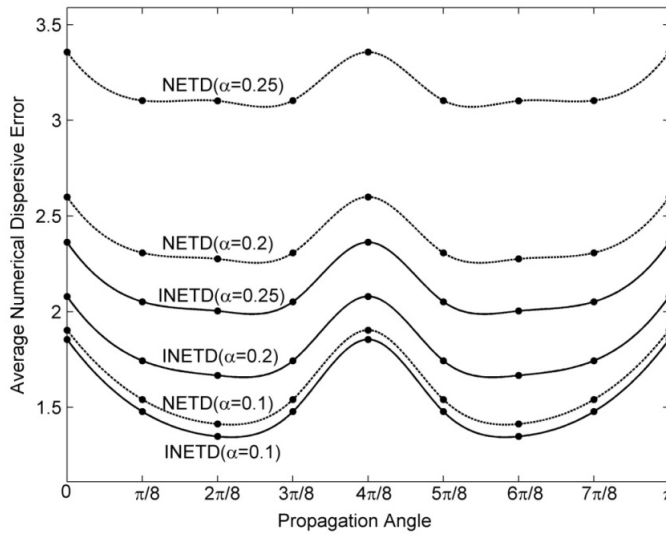


Fig. 2. The average numerical dispersive errors of the INETD (solid line) and the original NETD (dashed line) methods for different Courant numbers and propagation angles for the 2D Case.

ERROR ANALYSIS

To investigate the accuracy of the INETD method, we estimate the theoretical and relative numerical errors of the INETD method, and compare with the NETD method.

Theoretical analysis

Using the Taylor series expansion, we conclude that the INETD method is accurate third-order in time and fourth-order in space. Thus, the temporal accuracy of the INETD method is increased from second order in the original NETD method to third order, and the spatial accuracy remains the same as that of the original.

Numerical errors

To further illustrate the accuracy of the INETD method, in the following we compare the numerical errors caused by the INETD method and the original NETD method for the 2D acoustic wave equation.

We consider the following 2D initial value problem:

$$\left\{ \begin{array}{l} \frac{\partial^2 u}{\partial x^2} + \frac{\partial^2 u}{\partial z^2} = \frac{1}{c_0^2} \frac{\partial^2 u}{\partial t^2} \\ u(0, x, z) = \cos\left(-\frac{2\pi f_*}{c_0} \cdot \cos \theta_0 \cdot x - \frac{2\pi f_*}{c_0} \cdot \sin \theta_0 \cdot z\right) \\ \frac{\partial u(0, x, z)}{\partial t} = -2\pi f_* \sin\left(-\frac{2\pi f_*}{c_0} \cdot \cos \theta_0 \cdot x - \frac{2\pi f_*}{c_0} \cdot \sin \theta_0 \cdot z\right) \end{array} \right. , \quad (23)$$

where c_0 is the velocity of the plane wave, f_* is the frequency, and θ_0 is an incident angle at time $t=0$. Obviously, the analytical solution for the initial value problem (23) is

$$u(t, x, z) = \cos\left(2\pi f_* \left(t - \frac{x}{c_0} \cos \theta_0 - \frac{z}{c_0} \sin \theta_0\right)\right). \quad (24)$$

For comparison, we use the INETD and the original NETD methods to solve the initial value problem (23). In our numerical experiments, the parameters are chosen as follows: the computational domain $0 \leq x \leq 6$ km, $0 \leq z \leq 6$ km, the frequency $f_* = 30$ Hz, the acoustic velocity $c_0 = 4$ km/s, and the incident angle of the plane wave $\theta_0 = \pi/4$. The relative error for the 2D case is defined by

$$E_r(\%) = \left\{ \frac{\sum_{i=1}^N \sum_{j=1}^N [u_{i,j}^n - u(t_n, x_i, z_j)]^2}{\sum_{i=1}^N \sum_{j=1}^N [u(t_n, x_i, z_j)]^2} \right\}^{\frac{1}{2}} \times 100, \quad (25)$$

where $u_{i,j}^n$ is the numerical solution and $u(t_n, x_i, z_j)$ is the analytical solution. To avoid the effects of artificial reflections from the edges of the computational domain, in this numerical experiment we use the exact solution (24) of the initial value problem (23) at the artificial boundaries in each of the two methods.

Fig. 3 shows the computational results of the relative error E_r at different times for different spatial and temporal increments, where the two lines of E_r for the INETD and the original NETD methods are shown in a semi-log scale. From Fig. 3, we conclude that the numerical errors introduced by the INETD method measured by E_r are consistently less than those of the original NETD method.

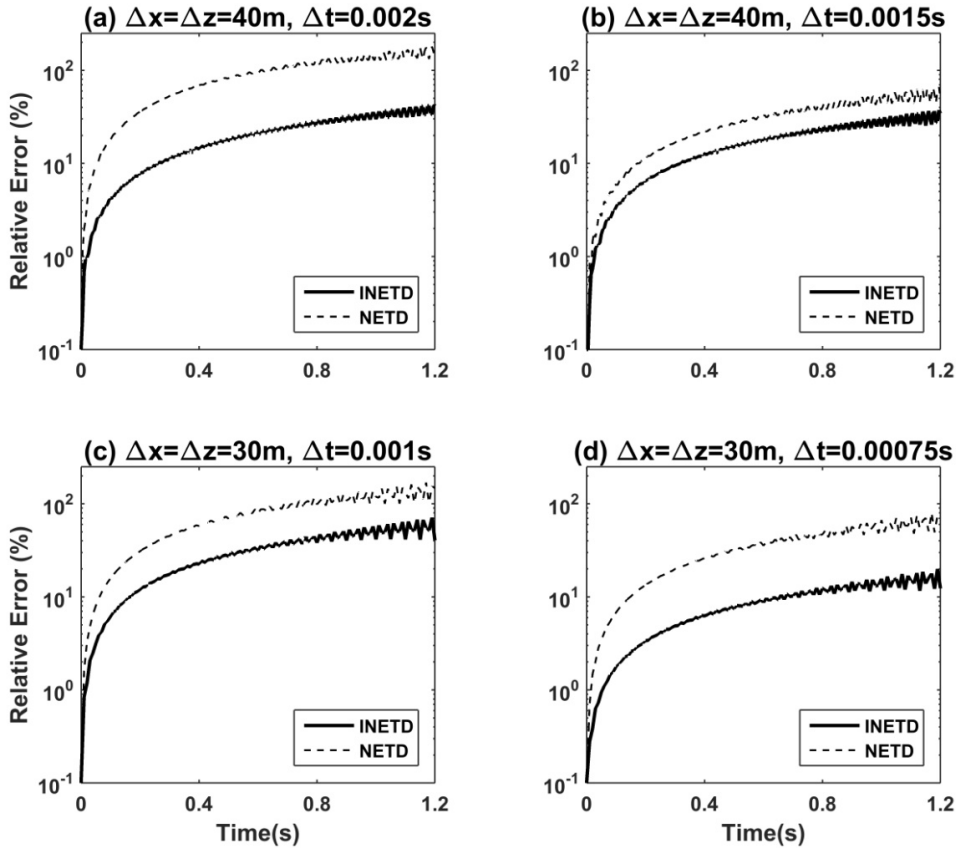


Fig. 3. The relative errors of the INETD and the original NETD methods measured by E_r [formula (25)] are shown in a semi-log scale for the 2D initial value problem (23). The spatial and temporal increments are **(a)** $\Delta x = \Delta z = 40$ m and $\Delta t = 0.002$ s, **(b)** $\Delta x = \Delta z = 40$ m and $\Delta t = 0.0015$ s, **(c)** $\Delta x = \Delta z = 30$ m and $\Delta t = 0.001$ s, **(d)** $\Delta x = \Delta z = 30$ m and $\Delta t = 0.00075$ s, respectively.

NUMERICAL DISPERSION AND EFFICIENCY

As shown above, the INETD method is superior in the numerical errors to NETD. The computational costs of the two methods are the same: for example, both took about 130 s to generate Fig. 3a, 173 s to generate Fig. 3b, 465 s to generate Fig. 3c, and 620 s to generate Fig. 3d. All the experiments in this work are done on a Core(TM)2 Duo CPU(2.40 GHz, 2.39 GHz) with 1.89 GB RAM. To investigate the ability of the INETD method to reduce numerical dispersion which is another important aspect characterizing numerical schemes, we compare the numerical solutions

generated by the INETD and the NETD methods, and by the fourth-order LWC method (Dablain, 1986) with the results from the analytic method (Aki and Richards, 1980) for the acoustic wave equation in a homogeneous medium model.

In this example, we choose a homogeneous medium with an acoustic velocity of $c_0 = 4$ km/s. The model size is $0 \leq x \leq 7.2$ km and $0 \leq z \leq 7.2$ km, and the source has a dominant frequency of $f_0 = 20$ Hz located at the center of the model, and the receiver is located at $(x = 4.2$ km, $z = 3.6$ km). The source time-function is a Ricker wavelet

$$f(t) = -5.76 f_0^2 \left(1 - 16(0.6 f_0 t - 1)^2\right) \exp\left(-8(0.6 f_0 t - 1)^2\right) \quad (26)$$

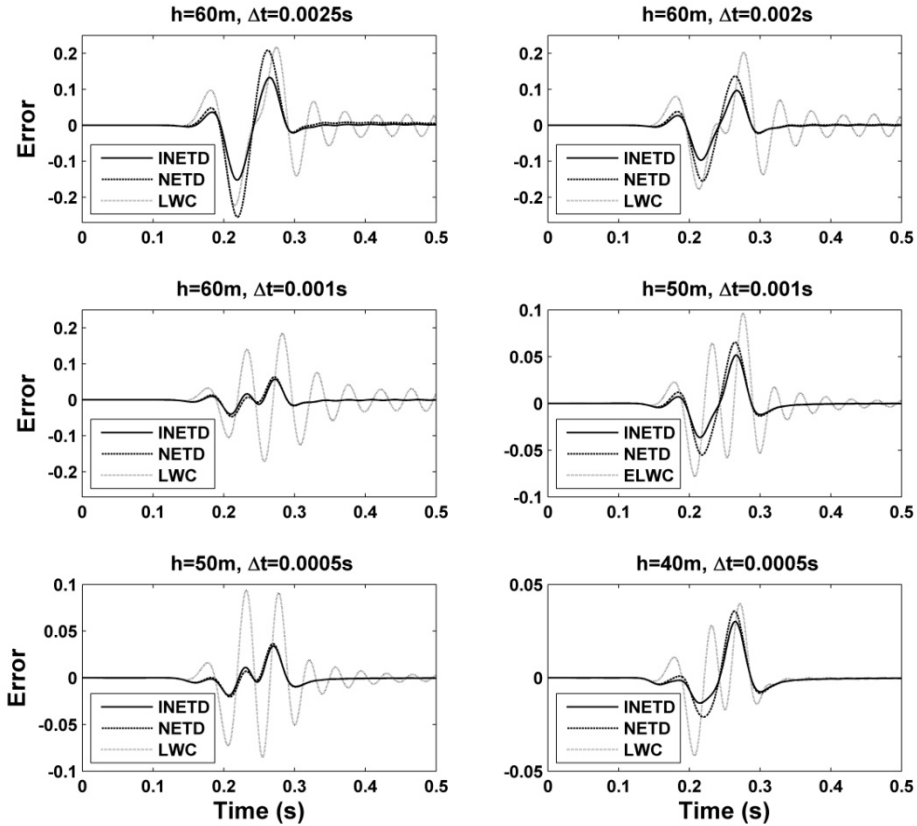


Fig. 4. Numerical errors of the INETD, the NETD and the LWC methods at the receiver. Note that these figures are plotted on different scales.

We choose the spatial increments $h = \Delta x = \Delta z = 60$ m, 50 m and 40 m, resulting in 3.3, 4 and 5 grid points per minimal wavelength, respectively.

Fig. 4 shows a comparison among the INETD, the NETD and the LWC methods made of their numerical error on the different spatial and temporal increments at the receiver.

From Fig. 4, we see that the INETD and the NETD methods have lower numerical dispersion than that of the fourth-order LWC method. And we observe that the errors and the numerical dispersion of the INETD are the smallest of the three methods. Meanwhile, the errors and the numerical dispersion of the INETD are gradually smaller as the spatial and temporal grid sizes decrease, indicating both the convergence and the validity of the INETD.

NUMERICAL EXAMPLES

In this section we present four numerical examples to investigate the validity of the INETD method. In all the experiments, the model parameters are the same as those used in Zhang et al. (2014), and the explosive source [eq. (26)] is used.

Example 1: Three-layer model

First we choose a computational domain of $0 \leq x \leq 6$ km and $0 \leq z \leq 6$ km and a three-layer model with the two horizontal interfaces at 2 km and 3.33 km depth, respectively. The velocity is 3.0 km/s in the top layer, 2.0 km/s in the middle layer, and 4.0 km/s in the bottom layer. The explosive source [eq. (26)] with a dominant frequency of $f_0 = 25$ Hz is located at the center of the domain and spatial and temporal increments are chosen as $\Delta x = \Delta z = 20$ m and $\Delta t = 5 \times 10^{-4}$ s, resulting in 4 grid points per minimum wavelength.

Fig. 5 shows the wavefield snapshots generated by INETD at four times; these show the wave propagation phenomena including reflection and transmission at the interfaces without visible numerical dispersion. This experiment demonstrates that INETD can deal well with models that contain strong velocity contrasts between the adjacent layers on coarse spatial grids.

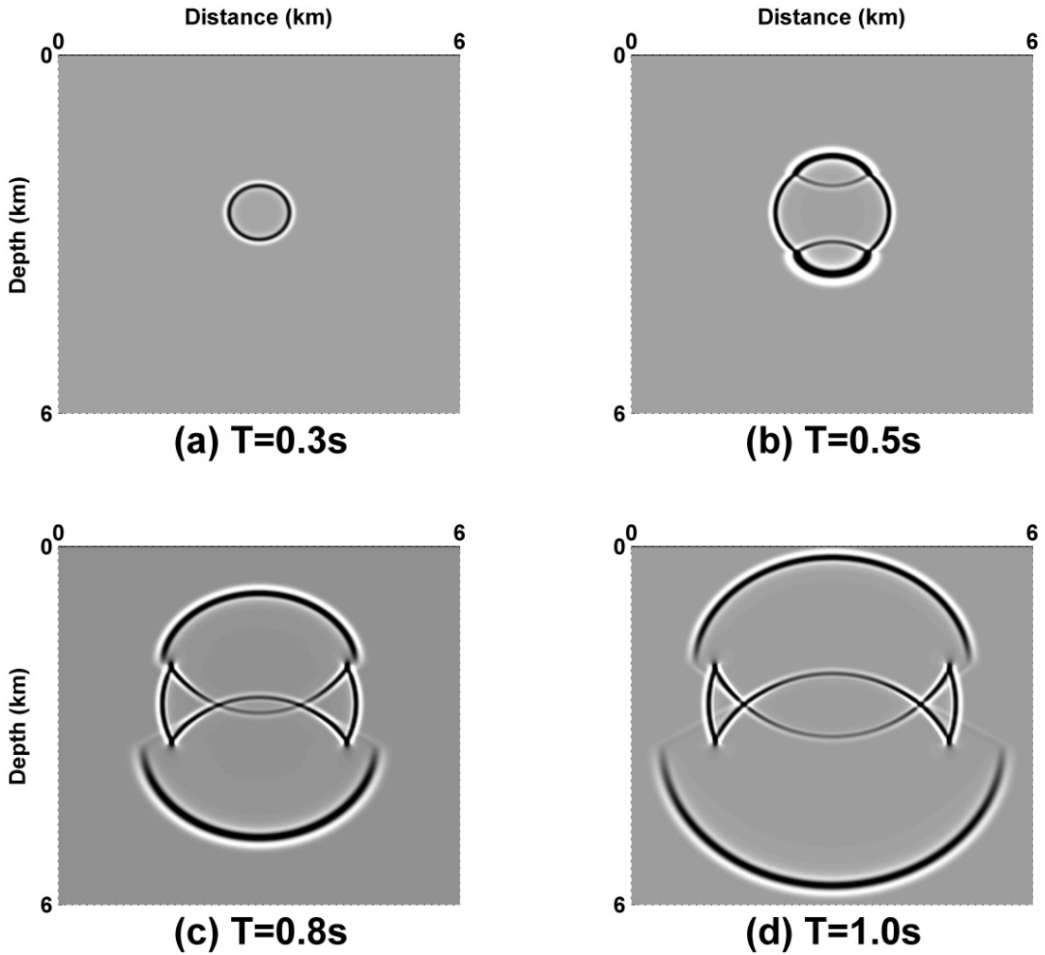


Fig. 5. Snapshots of acoustic wavefields at time **a** 0.3 s, **b** 0.5 s, **c** 0.8 s, and **d** 1.0 s for the three-layer model generated by the INETD method.

Example 2: Marmousi model

In the second experiment, we choose the Marmousi model (Versteeg and Grau, 1991) to demonstrate the performance of the INETD method in realistically complicated media. Fig. 6 shows the velocity structure $c(x, z)$, where the velocity varies from 1.5–5.5 km/s. We choose the spatial increments $\Delta x = \Delta z = 24$ m and the temporal increment $\Delta t = 0.000436$ s. The number of grid points is 384×122 so that the computational domain is

$0 \leq x \leq 9.192$ km and $0 \leq z \leq 2.904$ km. The source, which has a dominant frequency of $f_0 = 15$ Hz, is located in the middle on the surface, resulting in 4.17 grid points per minimal wavelength.

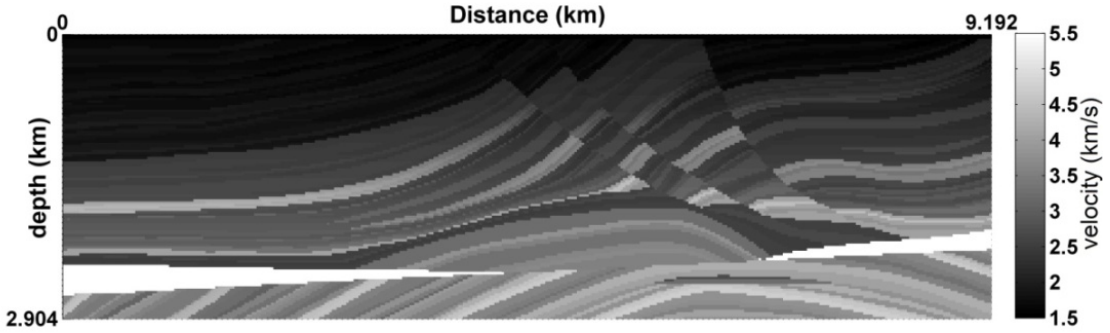


Fig. 6. The Marmousi model.

Fig. 7 shows the wavefield snapshots generated by the INETD at times $T = 0.6$ s, $T = 0.9$ s, $T = 1.2$ s, and $T = 1.5$ s, respectively; these snapshots are clean and have no visible numerical dispersion for the complicated geological model even though the spatial increment is large. In this experiment, we use the perfectly matched layer absorbing boundary condition (Komatitsch and Tromp, 2003; Ma et al., 2015) to treat the grid edges.

Example 3: a homogeneous elastic model

We consider the following elastic wave equations in a 2D homogeneous TI medium:

$$\begin{cases} \rho \frac{\partial^2 u}{\partial t^2} = c_{11} \frac{\partial^2 u}{\partial x^2} + (c_{13} + c_{44}) \frac{\partial^2 w}{\partial x \partial z} + c_{44} \frac{\partial^2 u}{\partial z^2} + f_1 \\ \rho \frac{\partial^2 w}{\partial t^2} = c_{44} \frac{\partial^2 w}{\partial x^2} + (c_{13} + c_{44}) \frac{\partial^2 u}{\partial x \partial z} + c_{33} \frac{\partial^2 w}{\partial z^2} + f_2 \end{cases}, \quad (27)$$

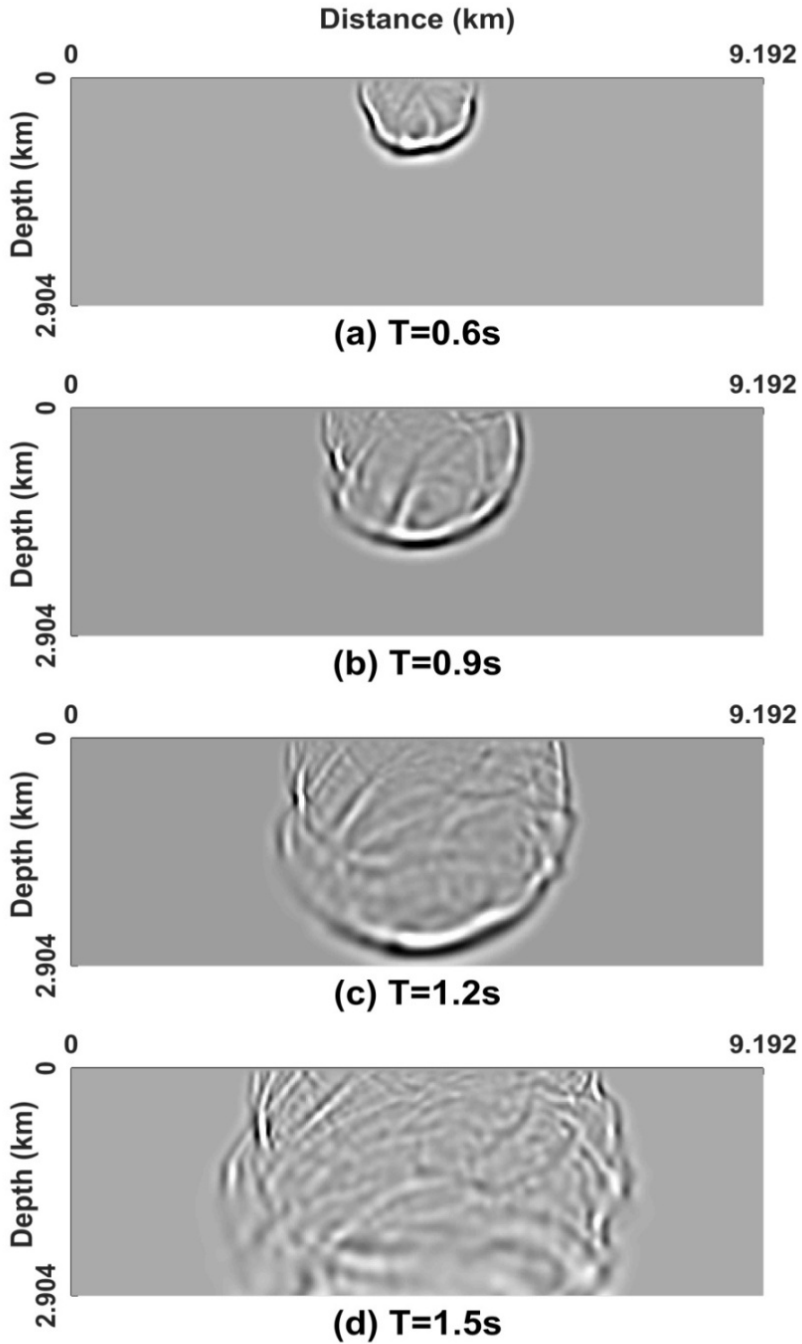


Fig. 7. Snapshots of acoustic wave fields at time **a** 0.6 s, **b** 0.9 s, **c** 1.2 s, and **d** 1.5 s for the Marmousi model generated, by the INETD method.

where u and w are the displacement components in the x - and z -directions, respectively. c_{11} , c_{13} , c_{33} and c_{44} are the elastic constants; ρ is the medium density; f_1 and f_2 are the source force components in the x - and z -directions. The computational parameters are $c_{11} = 45$, $c_{13} = 9.6$, $c_{33} = 37.5$, and $c_{44} = 12$ GPa, and $\rho = 1.0$ g/cm³. The mesh size is 401×401 points, the spatial grid increment is $\Delta x = \Delta z = 30$ m, and the time increment is $\Delta t = 0.00067$ s.

The source located at the center of the computational domain is a Ricker wavelet with a dominant frequency of $f_0 = 30$ Hz. Fig. 8 shows the x - and z -component snapshots at $T = 0.6$ s generated by the INETD method. The snapshots show clear wavefield information of the displacement without visible numerical dispersion. The cusps and the anisotropy of the velocity of the wave propagation can be clearly seen. In short, the numerical results demonstrate that the INETD method can simulate the elastic wave propagation effectively.

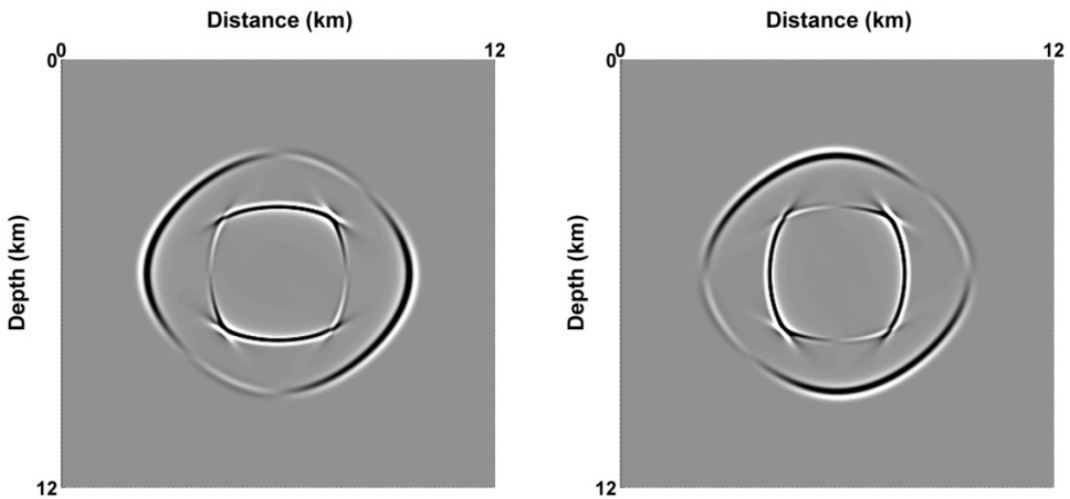


Fig. 8. Snapshots of elastic wave fields in the 2D homogeneous TI medium at time 0.6 s, generated by the INETD method for (left) the x -direction displacement component and (right) the z -direction displacement component.

Example 4: a two-layer elastic model

For this example, we choose a two-layer elastic model with large velocity contrasts across the interface. The size of the computational domain is $0 \leq x \leq 4$ km and $0 \leq z \leq 4$ km, and the horizontal interface of the two layers is at 2.4 km depth. The Lamé constants and densities of the two-layer model are $\rho_1 = 1.5 \text{ g/cm}^3$, $\lambda_1 = 1.5 \text{ GPa}$, $\mu_1 = 2.5 \text{ GPa}$ in the top layer, and $\rho_2 = 2.0 \text{ g/cm}^3$, $\lambda_2 = 11.0 \text{ GPa}$, $\mu_2 = 15.0 \text{ GPa}$ in the bottom layer. These correspond to the P - and SV -wave velocities of 1.63 and 1.29 km/s in the top layer, and 3.61 and 2.74 km/s in the bottom layer. The chosen spatial increment is $\Delta x = \Delta z = 15$ m, and the chosen temporal increment is $\Delta t = 0.0005$ s. The source, which has a frequency of $f_0 = 20$ Hz, is a symmetric Ricker wavelet located at $(x = 2 \text{ km}, z = 1.85 \text{ km})$.

Fig. 9 shows the x -direction and z -direction displacement snapshots at $T = 0.6$ s, generated by the INETD. The numerical results clearly show the elastic wave propagation phenomena in the two-layer model, which indicates that the INETD can also be used in a multilayer medium with strong interfaces for elastic wave propagation.

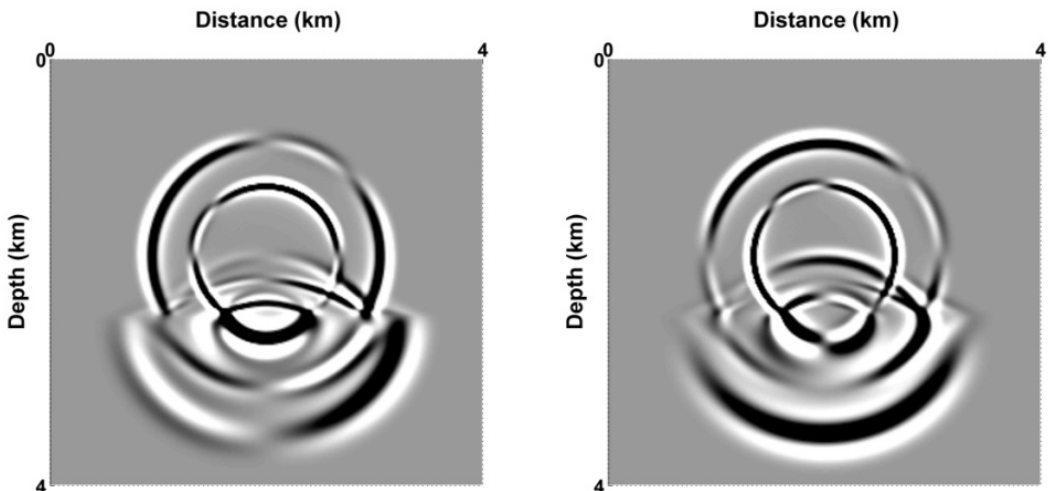


Fig. 9. Snapshots of elastic wavefields in the two-layer medium at time 0.6 s, generated by the INETD method for (left) the x -direction and (right) the z -direction displacement components.

ANOTHER CONSIDERATION OF THE INETD SCHEME

Now take a closer look at the INETD scheme (20). We can replace approximation (19) by the approximation

$$(\mathbf{I} - \mathbf{C})^{-1} \approx \mathbf{I} + \mathbf{C} + \mathbf{C}^2 + \mathbf{C}^3, \quad (28)$$

resulting in another INETD scheme as

$$\mathbf{Y}^{n+1} = (\mathbf{I} + \mathbf{C} + \mathbf{C}^2 + \mathbf{C}^3) \left(\exp(\mathbf{L}\Delta t) + \frac{1}{\Delta t} (\mathbf{L}^{-1})^2 (\mathbf{L}\Delta t \exp(\mathbf{L}\Delta t) - \exp(\mathbf{L}\Delta t) + \mathbf{I}) \mathbf{N} \right) \mathbf{Y}^n. \quad (29)$$

Table 3. The approximate maximum Courant numbers of the original and improved methods.

| Method | NETD | INETD1 | INETD2 |
|-----------------------------|--------|--------|--------|
| $\alpha_{\max}(1\text{-D})$ | 0.4132 | 0.5178 | 0.8263 |
| $\alpha_{\max}(2\text{-D})$ | 0.2583 | 0.3136 | 0.7811 |

Table 3 shows the approximate maximum Courant numbers of the NETD scheme (13), the INETD scheme (20) (INETD1) and the INETD scheme (29) (INETD2) for the 1D and 2D cases. From Table 3, we see that the INETD scheme (29) exhibits higher stability limits than the INETD scheme (20) and the NETD scheme (13). The INETD scheme (29) gives more accurate numerical results than the INETD scheme (20) and the NETD scheme (13) when the same grids are used. However, the INETD scheme (29) increases the computational cost by about 30% compared with the INETD scheme (20).

CONCLUSIONS

We have improved the original NETD for solving acoustic and elastic wave equations, and investigated in detail the properties of the INETD method, including its stability, numerical dispersion, and accuracy. The

INETD method, compared with the NETD method, has more relaxed stability. In 1D, the approximate maximum Courant number of the INETD method is increased from 0.4132 in the original NETD method to 0.5178 (for the INETD scheme (29) 0.8263), and in 2D, from 0.2583 to 0.3136 (for the INETD scheme (29) 0.7811). The INETD method increases the accuracy in time from the second order of the original NETD method to the third order, while keeping the spatial accuracy the same as the original NETD method. This conclusion is also verified by our numerical experiments of computing the relative error E_r , via formula (25) for the 2D case. In addition, the dispersion error of the INETD method for the 1D and 2D cases is less than that of the NETD method.

When using the same temporal and spatial increments, the computational costs and storage space of the INETD (20) and the NETD methods are the same, while the INETD scheme (29) increases the computational cost by about 30% compared with the NETD scheme. However, because the INETD scheme (29) has a much higher stability limit, higher order of temporal accuracy and lower dispersion than the NETD, it can lead to high computational efficiency.

Meanwhile, wavefield modelling illustrates that the improved method can effectively reduce numerical dispersion when too-coarse computation grids are used. The INETD method is related to the Lie group method.

ACKNOWLEDGEMENTS

We thank the editor and an anonymous reviewer for their detailed comments and helpful revisions that greatly improved this paper. We also thank Prof. Dinghui Yang for his fruitful suggestions that enabled us to highly improve the paper.

REFERENCES

- Aki, K. and Richards, P.G., 1980. Quantitative Seismology: Theory and Methods. W.H. Freeman and Co., San Francisco.
- Chen, S., Yang, D.H. and Deng, X.Y., 2010. A weighted Runge-Kutta method with weak numerical dispersion for solving wave equations. Commun. Comput. Phys., 7: 1027-1048.
- Dablain, M.A., 1986. The application of high-order differencing to the scalar wave equation. Geophysics, 51: 54-66.

- Fei, T. and Lerner, K., 1995. Elimination of numerical dispersion in finite difference modelling and migration by flux-corrected transport. *Geophysics*, 60: 1830-1842.
- Feng, L.L., Yang, D.H. and Xie, W., 2015. An efficient symplectic reverse time migration method using a local nearly-analytic discrete operator in acoustic transversely isotropic media with a vertical symmetry axis. *Geophysics*, 80(2): S103-S112.
- Fornberg, B., 1998. *A Practical Guide to Pseudospectral Methods*. Cambridge University Press, Cambridge.
- Hairer, E., Lubich, C.H. and Wanner, G., 2006. *Geometric Numerical Integration*. 2nd ed., Springer Verlag, Berlin.
- Huang, B.S., 1992. A program for two-dimensional seismic wave propagation by the pseudospectrum method. *Comput. Geosci.*, 18 : 289-307.
- Iserles, A., Munthe-Kaas, H., Norsett, S.P. and Zanna, A., 2000. Lie group methods. *Acta Numer.*, 9: 215-365.
- Kelly, K., Ward, R., Treitel, S. and Alford, R., 1976. Synthetic seismograms: a finite-difference approach. *Geophysics*, 41: 2-27.
- Komatitsch and Tromp, J., 2003. A perfectly matched layer absorbing boundary condition for the second-order seismic wave equation. *Geophys. J. Internat.*, 154: 146-153.
- Kosloff, D. and Baysal, E., 1982. Forward modeling by a Fourier method. *Geophysics*, 47: 1402-1412.
- Kosloff, D., Reshef, M. and Loewenthal, D., 1984. Elastic wave calculations by the Fourier method. *Bull. Seismol. Soc. Am.*, 74 : 875-891.
- Li, J.S., Yang, D.H., Wu, H. and Ma, X., 2017. A low-dispersive method using the high-order stereo-modeling operator for solving 2D wave equations. *Geophys. J. Internat.*, 210: 1938-1964.
- Li, J.S., Yang, D.H. and Liu, F.Q., 2013. An efficient reverse-time migration method using local nearly analytic discrete operator. *Geophysics*, 78(1): S15-S23.
- Liu, S.L., Yang, D.H., Lang, C., Wang, W.S. and Pan, Z.D., 2017. Modified symplectic schemes with nearly-analytic discrete operators for acoustic wave simulations. *Comput. Phys. Communicat.*, 213: 52-63.
- Lloyd, N., 1996. *Finite Difference and Spectral Methods for Ordinary and Partial Differential Equations*. Ph.D. thesis, Cornell University, Ithaca.
- Ma, X., Yang, D.H. and Liu, F., 2011. A nearly analytic symplectically partitioned Runge-Kutta method for 2-D seismic wave equations. *Geophys. J. Internat.*, 187: 480-496.
- Ma, X., Yang, D.H., Song, G.J. and Wang, M.X., 2014. A low-dispersive symplectic partitioned Runge-Kutta method for solving seismic wave equations - I. Scheme and theoretical analysis. *Bull. Seismol. Soc. Am.*, 104: 2206-2225.
- Ma, X., Yang, D.H. and Song, G.J., 2015. A low-dispersive symplectic partitioned Runge-Kutta method for solving seismic wave equations - II. Wave-field simulations. *Bull. Seismol. Soc. Am.*, 105: 657-675.
- Mizutani, H., Geller, R.J. and Takeuchi, N., 2000. Comparison of accuracy and efficiency of time domain schemes for calculating synthetic seismograms. *Phys. Earth Planet. Inter.*, 119 : 75-97.
- Moszo, P., Kristek, J. and Halada, L., 2000. 3-D fourth-order staggered-grid finite-difference schemes: stability and grid dispersion. *Bull. Seismol. Soc. Am.*, 90: 587-603.

- Munthe-Kaas, H., 1999. High order Runge-Kutta methods on manifolds. *Appl. Numer. Math.*, 29: 115-227.
- Robert, L.B., 1991. An Introduction to Lie Groups and Symplectic Geometry. Ph.D.thesis, Duke University, Park City.
- Tong, P., Yang D.H., Hua, B.L. and Wang, M.X., 2013. A high-order stereo-modeling method for solving wave equations. *Bull. Seismol. Soc. Am.*, 103: 811-833.
- Versteeg, R.J. and Grau, G., 1991. The Marmousi experience. Proc. EAGE workshop Practical Aspects of Seismic Data Inversion, Copenhagen, 1990.
- Wang, S.Q., Yang, D.H. and Yang, K.D., 2002. Compact finite difference scheme for elastic equations. *J. Tsinghua Univ.*, 42: 1128-1131 (in Chinese).
- Xie, W., Yang, D.H., Liu, F.Q. and Li, J.S., 2014. Reverse-time migration in acoustic VTI media using a high-order stereo operator. *Geophysics*, 79(3): WA3-WA11.
- Yang, D.H., Liu, E.R., Zhang, Z.J. and Teng, J.W., 2002. Finite-difference modelling in 2D anisotropic media using a flux corrected transport technique. *Geophys. J. Internat.*, 148: 320-328.
- Yang, D.H., Lu, M., Wu, R.S. and Peng, J. M., 2004. An optimal nearly analytic discrete method for 2D acoustic and elastic wave equations. *Bull. Seismol. Soc. Am.*, 94: 1982-1991.
- Yang, D.H., Tong, P. and Deng, X.Y., 2012. A central difference method with low numerical dispersion for solving the scalar wave equation. *Geophys. Prosp.*, 60: 885-905.
- Yang, D.H., Teng, J.W., Zhang, Z.J. and Liu, E., 2003. A nearly-analytic discrete method for acoustic and elastic wave equations in anisotropic media. *Bull. Seismol. Soc. Am.*, 93: 882-890.
- Yang, D.H., Peng, J.M., Lu, M. and Terlaky, T., 2006. Optimal nearly analytic discrete approximation to the scalar wave equation. *Bull. Seismol. Soc. Am.*, 96: 1114-1130.
- Yang, D.H., Song, G.J. and Lu, M., 2007. Optimally accurate nearly-analytic discrete scheme for wave-field simulation in 3D anisotropic media. *Bull. Seismol. Soc. Am.*, 97: 1557-1569.
- Yang, D.H., Wang, N., Chen, S. and Song, G.J., 2009. An explicit method based on the implicit Runge-Kutta algorithm for solving the wave equations. *Bull. Seismol. Soc. Am.*, 99: 3340-3354.
- Yang, D.H. and Wang, L., 2010a. A split-step algorithm with effectively suppressing the numerical dispersion for 3D seismic propagation modeling. *Bull. Seismol. Soc. Am.*, 100: 1470-1484.
- Yang, D.H., Song, G.J., Hua, B.L. and Henri, C., 2010b. Simulation of acoustic wave-fields in heterogeneous media: A robust method with automatically suppressing numerical dispersion for large grid steps. *Geophysics*, 75(3): T99-T110.
- Yang, D.H., Wang, M.X. and Ma, X., 2014. Symplectic stereomodeling method for solving elastic wave equations in porous media. *Geophys. J. Internat.*, 196: 560-579.
- Zhang, X., Yang, D.H. and Song, G.J., 2014. A nearly analytic exponential time difference method for solving 2D seismic wave equations. *Earthq. Sci.*, 27: 57-77.
- Zheng, H.S., Zhang, Z.J. and Liu, E.R., 2006. Non-linear seismic wave propagation in anisotropic media using the flux-corrected transport technique. *Geophys. J. Internat.*, 165: 943-956.